Technetium(III), Technetium(II), and Technetium(I) Complexes with Pyridine Ligands. Can Pyridine Coordination Stabilize the Low Oxidation States of Technetium?

Joseph Barrera,* Anthony K. Burrell,† and Jeffrey C. Bryan‡

MST-7, MS E549, Los Alamos National Laboratory, Los Alamos, New Mexico 87545

Received March 10, 1995[⊗]

The substitution chemistry of $TcCl_3(PPh_3)_2(CH_3CN)$ is rather facile relative to the analogous rhenium complex, since both the chloride and phosphine ligands are easily substituted for various pyridine ligands. Consequently a series of Tc^{III} complexes with amine, pyridine, and polypyridyl ligands were prepared and characterized by ^1H NMR and cyclic voltammetry. In addition, the zinc reduction of $TcCl_4(py)_2$ in the presence of pyridine results in $TcCl_2(py)_4$. Structural and spectroscopic data indicate that this Tc^{II} complex exhibits strong metal−pyridine interactions characteristic of low-valent amine complexes of Re^{II} and Os^{II}. For example, a decrease of 0.04 and 0.06 Å is observed for the *trans*-Tc−N bond length in $TcCl_2(py)_4$ relative to *mer*-$TcCl_3(pic)_3$ and $[TcCl_2(py)_3(PPh_3)]^+$, respectively. This ability of pyridine to function both as a strong σ-donor and moderate π-acid ligand has resulted in the isolation of technetium complexes in various oxidation states with similar ligand environments. As a result, a structural comparison of $[TcCl_2(py)_3(PPh_3)]^+$, $TcCl_2(py)_4$, $TcCl(tpy)(py)_2$, and other known Tc^{III} and Tc^{II} pyridine complexes is presented. Crystals of $[TcCl_2(py)_3(PPh_3)]PF_6$ are triclinic, with space group $P\bar{1}$, $Z = 2$, and lattice parameters $a = 12.677(4)$ Å, $b = 13.064(4)$ Å, $c = 13.103(5)$ Å, $\alpha = 110.14(3)°$, $\beta = 101.12(3)°$, $\gamma = 96.61°$, $V = 1959$ Å^3, and $R = 0.0615$ ($R_w = 0.1148$). Crystals of $TcCl_2(py)_4$ are tetragonal, with space group $I4_1/acd$, $Z = 8$, and lattice parameters $a = 15.641(4)$ Å, $c = 16.845(6)$ Å, $V = 4121$ Å^3, and $R = 0.0373$ ($R_w = 0.0290$). Crystals of $TcCl(tpy)(py)_2$ are orthorhombic, with space group $C222_1$, $Z = 4$, and lattice parameters $a = 9.359(3)$ Å, $b = 16.088(6)$ Å, $c = 18.367(4)$ Å, $V = 2765$ Å^3, and $R = 0.0499$ ($R_w = 0.0599$).

Introduction

Nearly 30 years ago the Wilkinson group reported the preparation and substitution chemistry of $ReCl_3(PPh_3)_2(CH_3CN)$.[1] Prior to this account the chemistry of Re^{III} was largely unexplored, and to some degree this is still true today. Until very recently[2] the coordination chemistry of Re^{III} was dominated by phosphine ligation,[3] in part due to the inherent difficulties with the ligand substitution chemistry of the acetonitrile complex above. For example, substitution of both PPh_3 ligands or even one of the chloride ligands is relatively difficult. Following the lead of rhenium, initial reports of Tc^{III} chemistry also focused on the synthesis and characterization of various complexes with phosphine ligands.[4] The one exception to this trend was the preparation of various $TcCl_3(py)_3$ complexes by Clarke et al. via phosphine reduction of $[TcOCl_4]^-$.[5] The recent report of $TcCl_3(PPh_3)_3(CH_3CN)$[6] has created a new avenue for exploring the chemistry of Tc^{III}. We envisioned the second-row cogener should exhibit a greater tendency toward ligand substitution and thus lead to Tc^{III} complexes with a variety of ligand environments.

Most of the known low-valent technetium complexes contain ligands which can function as moderate to strong π-acids, i.e. arylphosphines, isocyanides, carbon monoxide, or nitroysl.[7] However, our interest is to develop a coordinatively unsaturated, low-valent, *electron-rich* technetium metal center dominated by a very weak π-acid ligand environment. Such a complex should strongly back-bond to a variety of unsaturated substrates[8] and result in the development of unusual reaction chemistry.[9] Described here are several examples of mononuclear, octahedral Tc^{III}, Tc^{II}, and Tc^{I} complexes with predominantly polypyridyl ligand environments. The Tc^{III} complexes were prepared via the substitution chemistry of $TCl_3(PPh_3)_2(CH_3CN)$, and the Tc^{II} and Tc^{I} complexes were prepared by their subsequent reduction chemistry. In addition, the ability of pyridine to function as both a good σ-donor and a moderate π-acid ligand provides a rare structural comparison of a transition metal in three different oxidation states contained within a nearly identical ligand field.

Abbreviations. OTF = $CF_3SO_3^-$; DME = 1,2-dimethoxyethane; DMAc = *N*,*N*′-dimethylacetamide; TBAH = tetrabutylammonium hexafluorophosphate; Me_2Bpy = 4,4′-dimethylbipyridine; tpy = terpyridine; (*t*-butyl$_3$tpy) = 4,4′,4″-tris(*tert*-butyl)terpyridine; tmeda = tetramethylethylenediamine; py = pyridine.

Experimental Section

General Considerations. *Caution!* The isotope ^{99}Tc used in the syntheses of all technetium complexes described in this paper is a low-energy β^- emitter ($E_{max} = 0.29$ MeV) with a very long half-life (2.1×10^5 years). All experiments are performed in laboratories designated and approved for low-level radioactive materials following procedures and techniques described elsewhere.[10] Routine ^1H spectra were

* To whom correspondence should be addressed.
† Present address: Massey University, Palmerston North, New Zealand.
‡ Present address: Oak Ridge National Laboratory, MS 6119, Building 4500S, Oak Ridge, Tennessee 37831-6119.
⊗ Abstract published in *Advance ACS Abstracts,* December 1, 1995.

(1) Rouschias, G.; Wilkinson, G. *J. Chem. Soc. A* **1967**, 993.
(2) (a) Orth, S. D; Barrera, J.; Sabat, M.; Harman, W. D. *Inorg. Chem.* **1993**, *32*, 594. (b) Mayer, J. M.; Thorn, D. L.; Tulip, T. H. *J. Am. Chem. Soc.* **1985**, *107*, 7454.
(3) (a) Rouschias, G. *Chem. Rev.* **1974**, *74*, 531. (b) Chat, J.; Garforth, J. D.; Johnson, J. P.; Rowe, G. A. *J. Chem. Soc.* **1964**, 601.
(4) Libson, K.; Barnett, B. l.; Deutsch, E. *Inorg. Chem.* **1983**, *22*, 1695.
(5) Lu, J.; Yamano, A.; Clarke, M. *Inorg. Chem.* **1990**, *29*, 3483.
(6) Pearlstein, R. M.; Davies, W. M.; Jones, A. G.; Davison, A. *Inorg. Chem.* **1989**, *28*, 3332.
(7) $[Tc(tpy)_2]^+$, and $[Tc(bpy)_3]^+$ are exceptions to this trend. Archer, C. M.; Dilworth, J. R.; Kelly, J. D.; McPartlin, M. *Polyhedron* **1989**, *8*, 1879.
(8) Taube, H. *Pure Appl. Chem.* **1991**, 63.
(9) Burrell, A. K.; Bryan, J. C.; Kubas, G. J. *Organometallics* **1994**, *13*, 1067.

0020-1669/96/1335-0335$12.00/0

recorded on a Bruker 250 or a Bruker WM300 spectrometer and are reported in ppm shift from tetramethylsilane. Electrochemical experiments were performed under helium using a PAR model 362 potentiostat. Cyclic voltammograms were recorded (Kipp & Zonen BD90 XY recorder) in a standard three-electrode cell from +1.40 to −2.35 V with a glassy carbon working electrode. All potentials are reported vs NHE and, unless otherwise noted, were determined in DMAc (∼0.5 M TBAH) using ferrocene ($E_{1/2}$ = 0.55 V) in situ as a calibration standard. The peak-to-peak separation ($E_{p,a} - E_{p,c}$) was between 70 and 100 mV for all reversible couples reported unless otherwise noted. Elemental analyses were performed with a Perkin-Elmer 2400 CHN analyzer. UV−visible data were recorded in acetonitrile with a Perkin-Elmer Lambda 19. This work was performed in a helium atmosphere in a Vacuum Atmospheres Co. glovebox unless otherwise noted.

Crystallographic Studies. Unit cell constants were determined by least-squares refinement of the setting angles of a minimum of 25 unique reflections. Intensity data were obtained using $2\theta-\theta$ scans. All data were scaled for linear decay, and a semiempirical absorption correction (XEMP) based on the average relative intensity curve of azimuthal scan data was applied. The structures were solved using direct methods and refined with full-matrix least squares. Hydrogen atom positions were calculated (C−H = 0.96 Å) and added to the structure factor calculations without refinement. All calculations were performed using SHELXTL PLUS programs provided by Siemens Analytical. Crystallographic data are given in Table 6. Complete tabulations of crystallographic data, bond lengths and angles, atomic coordinates, thermal parameters, and completely labeled ball and stick diagrams are available as supporting information.

$[TcCl_2(py)_3(PPh_3)]PF_6\cdot(CH_2Cl_2)(C_6H_{14})_{1/2}$ (4). A yellow, block-shaped crystal, measuring 0.27 × 0.30 × 0.45 mm, was mounted on a glass fiber using silicone grease and placed in a cold stream (−40 °C) of an Enraf-Nonius CAD4 diffractometer. A total of 11 100 reflections ($4 \le 2\theta \le 50°$, $\pm h$, $\pm k$, $\pm l$) were collected. The hexane and CH_2Cl_2 lattice solvent molecules were disordered, with hexane being particularly difficult to model adequately. All non-hydrogen atoms, except disordered lattice solvent atoms, were refined anisotropically. Only the 5747 independent reflections with $F > 6\sigma_F$ were used in the refinement. Selected bond lengths and angles are given in Table 3, and selected atomic coordinates are given in Table 7.

$TcCl_2(py)_4$ (9). A purple, rod-shaped crystal, measuring 0.11 × 0.18 × 0.58 mm, was mounted on a glass fiber using silicone grease and placed in a cold stream (−70 °C) of a Siemens R3m/V diffractometer. A total of 4699 reflections ($4 \le 2\theta \le 56°$, $\pm h$, $\pm k$, $-l$) were collected. All non-hydrogen atoms were refined anisotropically. Only the 767 independent reflections with $F > 4\sigma_F$ were used in the refinement. Selected bond lengths and angles are given in Table 4, and atomic coordinates are given in Table 8.

$TcCl(tpy)(py)_2\bullet(C_7H_8)$ (10). A dark violet, plate-shaped crystal, measuring 0.05 × 0.13 × 0.23 mm, was mounted on a glass fiber using silicone grease and placed in a cold stream (−85 °C) of an Enraf-Nonius CAD4 diffractometer. A total of 2770 reflections ($4 \le 2\theta \le 50°$, h, $\pm k$, l) were collected. The pyridine ligand and the toluene lattice solvent molecule exhibit disorder over two sites (occupancy ratio roughly 1:1). All non-hydrogen atoms, except those part of a disordered group, were refined anisotropically. Only the 1611 independent reflections with $F > 4\sigma_F$ were used in the refinement. Selected bond lengths and angles are given in Table 5, and selected atomic coordinates are given in Table 9.

Solvents. All distillations were performed under nitrogen. Deuterated solvents were stirred in the presence of the appropiate drying agents and vacuum transferred. Acetone-d_6 and DMF-d_7 (Cambridge Isotopes) were used as received. Methylene chloride was refluxed over CaH_2 and distilled. Diethyl ether was refluxed over Na/benzophenone and distilled. DME was refluxed over Na and distilled. Acetonitrile was refluxed over CaH_2 and distilled. DMAc (Aldrich-anhydrous) was used as received. Acetone (Fluka) was deoxygenated prior to use. Pyridine (Fluka-anhydrous) was used as received.

Materials. Ammonium pertechnetate was obtained from the Oak Ridge National Laboratory and was purified as described previously.[4] $TcCl_3(PPh_3)_2(CH_3CN)$ was prepared according to the literature.[6] $TcCl_4(py)_2$ was prepared from a mixture of $(PPh_3H)_2[TcCl_6]$, $(PPh_3H)[TcCl_5(PPh_3)]$, and $TcCl_4(PPh_3)_2$ according to the literature.[11]

$[TcCl_2(Me_2Bpy)_2]OTf$. $TcCl_3(PPh_3)_2(CH_3CN)$ (0.25 g, 0.35 mmol) and Me_2Bpy (0.24 g, 1.31 mmol) were added to a 25 mL flask and suspended in DME (10 mL). The TlOTf (0.13 g, 0.37 mmol) was added, and the reaction was heated in an oil bath (70 °C) for 4 h. The reaction was refluxed for an additional 30 min and cooled to room temperature. The resulting purple solid was collected and extracted with methylene chloride/acetone (4/1, 4 × 2 mL), and the extracts were filtered through Celite. The solvent volume was partially reduced in vacuo, and OEt_2 was slowly added. The resulting suspension was stirred for $1^1/_2$ h, and following filtration the purple solid was washed with OEt_2 (2 mL) and dried in vacuo, 0.16 g, 67%. ^{1}H NMR (acetone-d_6): 47.33 (s, 2H), 43.71 (s, 6H), 34.75 (s, 6H), 33.46 (s, 2H), 26.81 (s, 2H), 7.07 (s, 2H), 5.48 (s, 2H), −4.45 (s, 2H). CV (100 mV/s; DMAc; TBAH): $E_{1/2}$ = 1.13, −0.16, −1.11 V vs NHE. Anal. Calcd for $TcC_{33}H_{24}N_4Cl_3O_3SF_3$: C, 43.74; H, 3.52; N, 8.16. Found: C, 43.88; H, 3.58; N, 8.30.

$[TcCl_2(PPh_3)(py)_3]OTf$. $TcCl_3(PPh_3)_2(CH_3CN)$ (0.17 g, 0.22 mmol) was suspended in a DME/pyridine solution (8 mL, 3/1). TlOTf (0.08 g, 0.23 mmol) was added, and the reaction mixture was heated in an oil bath (70 °C) for 2 h. The reaction was cooled to room temperature, the reaction mixture was filtered through Celite, and the solvents were removed in vacuo. The resulting orange oil was suspended in CH_2Cl_2 (7 mL), and the solution was filtered through Celite. OEt_2 (5 mL) was added to the stirred filtrate, followed by the slow addition (30 min) of hexanes (4 mL). The resulting yellow-orange solid was collected, washed with OEt_2, and dried in vacuo, 0.09 g. An additional 0.03 g was isolated upon cooling (−30 °C) of the filtrate, 66%. X-ray quality crystals were obtained from a cooled CH_2Cl_2/OEt_2/hexane solution. ^{1}H NMR (CD_2Cl_2): 20.61 (d, 2H), 18.07 (s, 6H), 15.73 (d, 2H), 10.76 (t, 3H), 8.22 (s, 6H), 2.98 (1H, t), 1.42 (s, 4H), −6.26 (br s, 4H), −18.13 (br s, 2H). CV (100 mV/s; DMAc; TBAH): $E_{1/2}$ = 0.86, −0.53 V vs NHE. Anal. Calcd for $TcC_{34}H_{30}N_3Cl_2PO_3SF_3$: C, 49.95; H, 3.70; N, 5.14. Found: C, 49.76; H, 3.75; N, 4.97.

$TcCl_3(PPh_3)(tmeda)$. $TcCl_3(PPh_3)_2(CH_3CN)$ (0.22 g, 0.28 mmol) was suspended in a DME solution (3 mL) containing tmeda (0.07 g). Toluene was added (4 mL), and the reaction mixture was heated in an oil bath at 80 °C for $2^1/_2$ h. During this time, the color of the reaction mixture turned from an orange to a yellow suspension. After cooling to room temperature, the solid was collected, washed with DME (1 mL) and OEt_2 (1 mL), and dried in vacuo, 0.15 g, 92%. ^{1}H NMR (CD_2Cl_2): 19.33 (6H, s), 11.54 (3H, s), 7.91 (6H, s), 1.62 (6H, s), −22.04 (6H, s). CV (100 mV/s; DMAc; TBAH): $E_{1/2}$ = 0.71, $E_{p,c}$ = −0.79 V vs NHE. Anal. Calcd for $TcC_{24}H_{31}N_2Cl_3P$: C, 49.46; H, 5.36; N, 4.81. Found: C, 49.22; H, 5.14; N, 4.65.

$TcCl_3(tpy)$. $TcCl_3(PPh_3)_2(CH_3CN)$ (0.15 g, 0.19 mmol) and 2,2′,2″-terpyridine (0.05 g, 21 mmol) were suspended in DME (10 mL). The reaction mixture was heated in an oil bath at 40−60 °C for 2 h and then heated at reflux for an additional 30 min. The reaction mixture was cooled to room temperature, and the black/green solid was collected, washed with DME (1 mL) and OEt_2 (2 × 1.5 mL), and dried in vacuo, 0.08g, 97%. The solid is insoluble in methylene chloride, acetone, acetonitrile, or benzene, but slightly soluble in *N*,*N*′-dimethylacetemide. CV (100 mV/s; DMAc; TBAH): $E_{1/2}$ = 0.67, −0.34 V, $E_{p,c}$ = −1.42 V; (100 mV/s; CH_2Cl_2; TBAH): $E_{1/2}$ = 0.73, −0.25 V vs NHE. Anal. Calcd for $TcC_{15}H_{11}N_3Cl_3$: C, 41.17; H, 2.53; N, 9.60. Found: C, 41.36; H, 2.85; N, 9.68.

$TcCl_3$(*t*-butyl$_3$tpy). $TcCl_3(PPh_3)_2(CH_3CN)$ (0.15 g, 0.19 mmol) and 4,4′,4″-tris(*tert*-butyl)terpyridine (0.09 g, 0.21 mmol) were suspended in DME (10 mL). The reaction mixture was heated in an oil bath at 60 °C for 2 h and then heated to reflux for an additional 30 min. The reaction mixture was cooled to room temperature, and the black/green solid was collected, washed with DME (2 mL) and OEt_2 (2 mL), and dried in vacuo, 0.077g, 96%. Analytically pure material was obtained by suspending the solid in toluene at 50 °C followed by filtration. The solid is insoluble in acetonitrile, acetone, benzene, or *N*,*N*′-dimethylacetemide, but slightly soluble in methylene chloride. CV (100 mV/s;

(10) Bryan, J. C.; Burrell, A. K.; Miller, M. M.; Smith, W. H.; Burns, C. J.; Sattelberger, A. J. *Polyhedron* **1993**, *12*, 1769−77.

(11) Breikss, A. I.; Davison, A.; Jones, A. G. *Inorg. Chim. Acta* **1990**, *170*, 75.

CH_2Cl_2; TBAH): $E_{1/2}$ = 0.60, −0.43 V vs NHE. Anal. Calcd for $TcC_{27}H_{35}N_3Cl_3$: C, 53.52; H, 5.82; N, 6.93. Found: C, 53.92; H, 5.53; N, 6.59.

[TcCl$_2$(py)$_4$]OTf. [TcCl(py)$_3$(PPh$_3$)]OTf (0.070 g, 0.85 mmol) was dissolved in pyridine (5 mL), and the reaction solution was refluxed for 2 h. The yellow-orange solution turned deep red in color during this time. The reaction was cooled to room temperature, and the pyridine was partially removed in vacuo to ∼1 mL. The residue was dissolved in CH_2Cl_2 (2 mL), and OEt_2 was added dropwise (5 mL). The resulting suspension was stirred for 10 min and filtered. The pale-orange solid was washed with OEt_2/CH_2Cl_2 (3/1, 2 × 0.5 mL) and dried under vacuum, 0.037 g, 68%. ^{1}H NMR (CD_2Cl_2): 20.56 (s, 8H), −1.96 (s, 4H), −13.68 (br s, 8H). CV (100 mV/s; DMAc; TBAH): $E_{1/2}$ = 1.34, −0.38, and −1.33 V vs NHE. Anal. Calcd for $TcC_{21}H_{20}N_4Cl_2O_3SF_3$: C, 39.76; H, 3.18; N, 8.83. Found: C, 39.45; H, 3.21; N, 8.72.

TcCl$_2$(py)$_4$. $TcCl_4(py)_2$ (0.73 g, 1.83 mmol) was suspended in pyridine (14 mL), and Zn powder was added (0.42 g). The reaction mixture was stirred at room temperature for 3 h and then was filtered through Celite. The deep violet-blue filtrate was reduced to approximately 8 mL in vacuo, and hexanes (8 mL) were slowly added over a period of 15 min. The resulting precipitate (L_nZnCl_x) was collected and discarded, since electrochemical data suggested only trace amounts of $TcCl_2(py)_4$. The resulting purple filtrate was concentrated in vacuo to an oily purple residue. This was extracted into CH_2Cl_2/OEt_2 (3/1, 3 × 4 mL), and the extracts were filtered through Celite. The filtrate was passed through a column of alumina measuring 0.8 × 4 cm. The purple elutant was concentrated, and upon the slow addition of hexanes a precipitate formed. This was collected, washed with OEt_2, and dried in vacuo, 0.21 g. The bronze solid atop the Celite (from the first filtration) was extracted into CH_2Cl_2/OEt_2 (3/1, 6 × 4 mL), and the extracts were passed through a column of alumina measuring 0.8 × 6 cm. The purple elutant was treated as above, 0.38 g, total 0.59 g, 67%. CV (100 mV/s; DMAc; TBAH): $E_{1/2}$ = 1.34, −0.38, and −1.33 V vs NHE. Anal. Calcd for $TcC_{20}H_{20}N_4Cl_2$: C, 49.50; H, 4.15; N, 11.54. Found: C, 49.86; H, 4.03; N, 11.41.

[TcCl(py)$_5$]BPh$_4$. $TcCl_2(py)_4$ (0.054 g, 0.11 mmol) and $NaBPh_4$ (0.040 g, 0.11 mmol) were dissolved in pyridine (6 mL) and heated to reflux for 2 h. The reaction color changed from violet to a red-purple during this time, and electrochemical data indicated approximately 95% conversion of $TcCl_2(py)_4$. The reaction mixture was cooled slightly, and the pyridine was removed in vacuo to give a red-purple oil. This residue was extracted with THF (2 × 4 mL), and the collected extracts were filtered through Celite. Slow addition of hexanes to the filtrate resulted in a dark red precipitate, 0.063 g, 65%. CV (100 mV/s; DMAc; TBAH): $E_{1/2}$ = 1.34, −0.38, and −1.33 V vs NHE.

TcCl(tpy)(py)$_2$ and [Tc(tpy)(py)$_3$]Cl. $TcCl_3$(tpy) (0.17 g, 0.39 mmol) was suspended in DME (1.5 mL), pyridine (3 mL), and Zn dust (1.15 g). The reaction mixture was stirred at room temperature for 2 h and then filtered through Celite. The solids remaining in the reaction vial were suspended with DME/pyridine (2/1, 4 × 1 mL), and the washings were filtered. The solvent was removed in vacuo, resulting in a viscous, purple liquid. This liquid was extracted into toluene at room temperature (2 × 10 mL), and the resulting suspension was filtered. The solids were washed with toluene (2 × 1.5 mL) and OEt_2 (1 × 2 mL) and dried in vacuo, 0.124 g. Electrochemistry indicated this solid was approximately 75% [Tc(tpy)(py)$_3$]Cl and 25% [TcCl(tpy)(py)$_2$]Cl. The toluene filtrate was placed in a freezer (−35 °C) overnight, and the resulting purple solution decanted from the small amount of solids present. Hexanes was added to the toluene, and the solution was returned to the freezer for 3 days. The resulting dark purple solid was collected, washed with toluene (1 × 1.5 mL) and OEt_2 (2 × 1.5 mL), and dried in vacuo, 0.038 g. Cyclic voltammetry indicates this solid to be approximately 95% TcCl(tpy)(py)$_2$ and 5% [Tc(tpy)(py)$_3$]Cl. X-ray quality crystals of TcCl(tpy)(py)$_2$ were obtained from a cooled (−40 °C) toluene/hexane solvent mixture.

Results

Syntheses. Reaction of $TcCl_3(PPh_3)_2(CH_3CN)$ (**1**) with tetramethylethylenediamine (tmeda) in DME results in substitution of the nitrile and one of the two phosphines by the bidentate amine ligand. Similar to that of known octahedral, Re^{III} chemistry,[2a] $TcCl_3(PPh_3)$(tmeda) (**2**) exhibits a Knight-shifted ^{1}H NMR spectrum from 20 to −20 ppm. The plane of symmetry in the molecule prevents the determination as to whether the chlorides are in a meridonal or facial geometry. The analogous reaction of $TcCl_3(PPh_3)_2(CH_3CN)$ with ethylenediamine also results in a yellow powder; however, the ^{1}H NMR spectrum and the cyclic voltammetric data *do not* suggest the formation of $TcCl_3(PPh_3)$(en). Reaction of **1** with TlOTf in the presence of a slight excess of Me_2Bpy or pyridine in DME results in the Tc^{III} cationic complexes, *cis*-[$TcCl_2$(MeBpy)$_2$]OTf (**3**) and *trans*-[$TcCl_2(PPh_3)(py)_3$]OTf (**4**), respectively. As for $TcCl_3(PPh_3)$(tmeda), both complexes exhibit well-defined Knight-shifted ^{1}H NMR spectra. Reaction of **1** with terpyridine or 4,4′,4″-tris(*tert*-butyl)terpyridine in refluxing DME results in the neutral $TcCl_3$(tpy) (**5**) and $TcCl_3$(*t*-butyl$_3$-tpy) (**6**), respectively. Unfortunately, both terpyridine complexes exhibit very limited solubility in all common organic solvents. The reaction of **1** in refluxing pyridine results in $TcCl_3(py)_3$ (**7**).[5] In addition, the reaction of *trans*-[$TcCl_2(PPh_3)$-(py)$_3$]OTf in refluxing pyridine results in pyridine substitution of the second triphenylphosphine ligand to form [$TcCl_2(py)_4$]-OTf (**8**). Complex **8** can also be prepared directly from **1** and TlOTf under similar reaction conditions. A synthetic summary for the above complexes is shown in Scheme 1.

Scheme 1. Substitution Chemistry of $TcCl_3(PPh_3)_2(CH_3CN)$

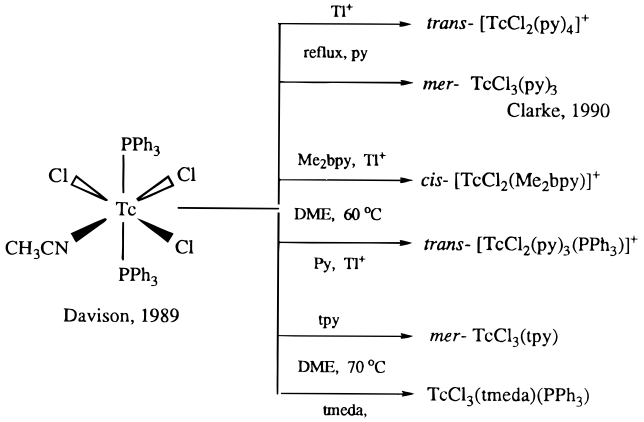

The zinc reduction of $TcCl_4(py)_2$ in pyridine results in the isolation of the neutral complex, $TcCl_2(py)_4$ (**9**). As expected this Tc^{II} complex *does not* exhibit a well-defined ^{1}H NMR spectrum; however, the material is easily characterized by cyclic voltammetry (*vide infra*). The $Tc^{II/I}$ couple is observed at −1.33 V vs NHE; however, our initial attempts to reduce this complex in an ultrasound bath at 60 °C with an excess of precleaned magnesium powder in the presence of acetone, dinitrogen, or benzaldehyde results in the recovery of $TcCl_2(py)_4$. The substitution chemistry of $TcCl_2(py)_4$ is surprisingly difficult, since prolonged heating in refluxing DME/bpy or refluxing CH_3-CN results in no change in the cyclic voltammogram of the reaction mixture. However, electrochemical evidence was observed for the substitution of a chloride ligand for a fifth pyridine in the presence of Na^+.

The zinc reduction of $TcCl_3$(tpy) in the presence of pyridine results in a product mixture containing *trans*-TcCl(tpy)(py)$_2$ (**10**), [Tc(tpy)(py)$_3$]Cl (**11**), and [TcCl(tpy)(py)$_2$]$^+$ (**12**). A partial seperation of these three complexes is achieved by toluene extraction followed by multiple recrystallizations from a toluene/hexane solvent mixture. Interestingly, dissolution of **11** in THF/toluene results in the slow conversion to **12** after several hours as evidenced by cyclic voltammetry. This oxidation process was observed with three distinct mixtures of **11** and **12** and is

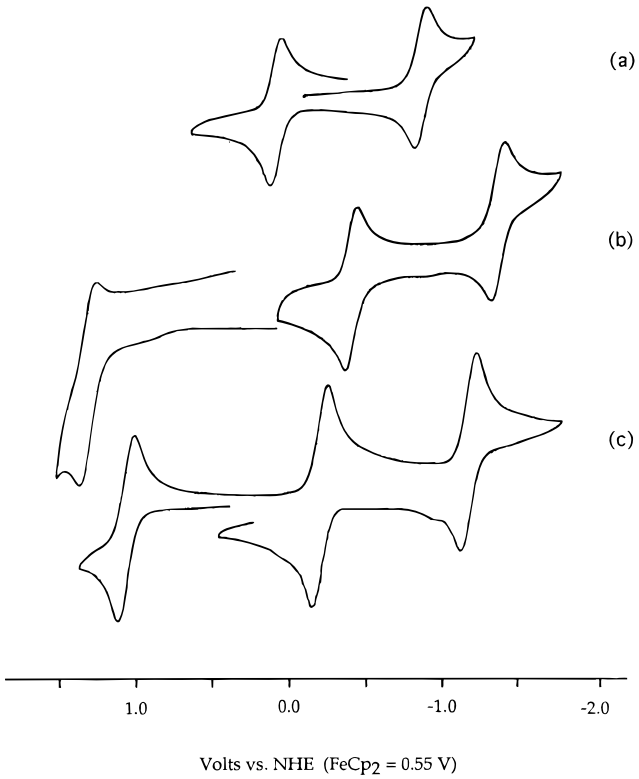

Figure 1. Cyclic voltammetric scans of (a) $TcCl(py)_5]BPh_4$, (b) $TcCl_2(py)_4$, and (c) $TcCl_2(Me_2bpy)_2]OTf$ in DMAc (TBAH) at 100 mV/s.

best explained by the presence of trace dioxygen within the helium-rich atmosphere. In addition, an attempt to isolate $TcCl(tpy)(py)_2$ (**10**) from a pyridine/DME solution containing a 4/1 mixture of **10**/**11** by precipitation with OEt_2/hexanes results in the quantitative isolation of $[Tc(tpy)(py)_3]Cl$ (**11**). Such an observation can only be explained in terms of a solution equilibrium between **10** and **11**, which is shifted completely to the latter due to precipitation of the less soluble chloride salt.

The Tc^{III} complexes, **1**−**8**, and $TcCl_2(py)_4$ are extremely stable toward hydrolysis. These complexes along with a small amount of ferrocene were dissolved in either acetone or acetonitrile, and two pipet drops of water were added. The solutions were then warmed to 50 °C over a 2 day period. No change in the cyclic voltammograms of these solutions was observed during this time with the exception of **5**.

Electrochemistry. The electrochemistry of the Tc^{III} polypyridyl complexes reported here is similar to that of the corresponding rhenium complexes.[12] That is, at least two metal-centered, reversible couples are observed for each of the complexes; see Figure 1 and Table 1. As expected, the $Tc^{III/II}$ couple becomes more positive as the amine ligand is varied from tmeda < py < Me_2bpy < tpy. For example, a difference of 220 V (55 mV/py) is observed for the substitution of four pyridine ligands with two 4,4′-dimethylbipyridine ligands, while a difference of 450 mV (150 mV/py) is observed for the substitution of three pyridine ligands with terpyridine. In addition, an interesting observation is the comparison of the redox behavior between $[TcCl_2(py)_4]^+$ and $[TcCl_2(PPh_3)(py)_3]^+$. Surprisingly, a *positive* shift in both the IV/III and III/II potentials is observed, 0.48 and 0.15 V, respectively, as the triphenylphosphine ligand is substituted for a fourth pyridine ligand. Such a shift is counterintuitive since triphenylphosphine is in general believed to be a stronger π-accepting and weaker σ-donor ligand than pyridine. For example, Lever assigns ligand parameters of 0.99, 0.39, and 0.25 for carbon monoxide, triphenylphosphine, and pyridine, respectively.[13] Substitution of chloride by pyridine results in an increase in redox potential of approximately 0.4 V per pyridine. This observation is virtually independent of oxidation state, since Tc^{III}, Tc^{II}, and Tc^{I} pyridine complexes all exhibit comparable shifts in redox potentials upon substitution. For example, the $Tc^{II/I}$ couple for $TcCl_3(py)_3$ vs $[TcCl_2(py)_4]^+$ and $TcCl(tpy)(py)_2$ vs $[Tc(tpy)(py)_3]^+$ both exhibit a shift of 0.39 V upon substitution of a chloride for a pyridine ligand. In addition, the $Tc^{III/II}$ and $Tc^{II/I}$ couples exhibit a shift of 0.47 and 0.49 V, respectively, upon substitution of a chloride for a pyridine ligand in $TcCl_2(py)_4$.

Table 1. Electrochemical Data for Technetium Amine Complexes[a]

complex	IV/III	III/II	II/I	ligand
$TcCl_3(PPh_3)_2(CH_3CN)$ (**1**)	1.00	−0.49	−2.00[c]	
$TcCl_3(PPh_3)$(tmeda)[b] (**2**)	0.71	−0.79[c]		
$TcCl_3(py)_3$ (**7**)	0.79	−0.79	−1.72[c]	
$TcCl_3$(tpy) (DMAc) (**5**)	0.67	−0.34	−1.42[c,d]	
(CH_2Cl_2)	0.73	−0.25		
$TcCl_3$(*t*-butyl$_3$tpy)[b] (**6**)	0.60	−0.43		
$[TcCl_2(Me_2Bpy)_2]OTf$ (**3**)	1.13	−0.16	−1.11	
$[TcCl_2(PPh_3)(py)_3])OTf$ (**4**)	0.86	−0.53[e]		
$[TcCl_2(py)_4]OTf$ (**8**)	1.34	−0.38	−1.33	
$TcCl_2(py)_4$ (**9**)	1.34	−0.38	−1.33	
$[TcCl(py)_5]BPh_4$		0.09	−0.84	
$[Tc(tpy)(py)_3]Cl$ (**11**)		0.70[f]	−0.43	−1.63
$TcCl(tpy)(py)_2$ (**10**)		0.41[f]	−0.82	−1.95

[a] Cyclic voltammetric data was obtained in DMAc at a scan rate of 100 mV/s unless otherwise noted and is reported in volts vs NHE (in situ reference: $FeCp_2^{0/+}$ = 0.55 V). [b] Cyclic voltammetric data was obtained in CH_2Cl_2. [c] Value reported is for an irreversible cathodic peak, $E_{p,c}$. [d] Multielectron process. [e] The redox couple shows partial irreversibility. [f] Value reported is for an irreversible anodic peak, $E_{p,a}$.

Table 2. UV−Visible Data for Technetium Amine Complexes

complex	λ_{max}, nm (cm^{-1})	ϵ M^{-1} cm^{-1}
$[TcCl_2(Me_2bpy)_2]OTf$ (**3**)	549 (18 210)	3 040
	376 (26 600)	4 260
	290 (34 480)	35 580
	248 (40 320)	23 740
$TcCl_3(py)_3$ (**7**)	407 (24 570)	6 250
	318 (31 450)	7 000
	286 (34 950)	12 680
	253 (39 530)	13 500
$[TcCl_2(py)_4]OTf$ (**8**)	363 (27 550)	2 850
	279 (35 840)	6 490
	253 (39 500)	8 600
$TcCl_2(py)_4$ (**9**)	538 (18 590)	13 600
	487 (20 530)	12 500
	435 (22 990)	10 100
	252 (39 680)	16 400

UV−Visible Spectra. The Tc^{III} pyridine complexes, $[TcCl_2(py)_4]^+$ and $TcCl_3(py)_3$, both exhibit two strong transitions between 250 and 290 nm and a shoulder to higher energy is observed in the higher energy transition; see Table 2. Relatively broad absorption peaks at 363 and 407 nm are observed in $[TcCl_2(py)_4]^+$ and $TcCl_3(py)_3$, respectively. On the other hand, the UV−visible spectrum of $[TcCl_2(py)_3(PPh_3)]^+$ is relatively featureless; however, a broad absorption is observed near 410 nm, which spreads into the higher energy bands below 260 nm. The latter are also not clearly resolved. The complex $[TcCl_2(Me_2bpy)_2]^+$ exhibits a spectrum very similar to Ru^{II} bipyridine complexes.[14] Two strong $\pi-\pi^*$ transitions localized on the bipyridine ligand are observed in the UV region at 248 and

(12) Orth, S. D.; Sabat, M.; Harman, W. D. Unpublished results.

(13) Lever, A. B. P. *Inorg. Chem.* **1990**, *29*, 1271.

(14) Bryant, G. M.; Fergusson, J. E.; Powell, H. K. J. *Aust. J. Chem*. **1971**, *24*, 257.

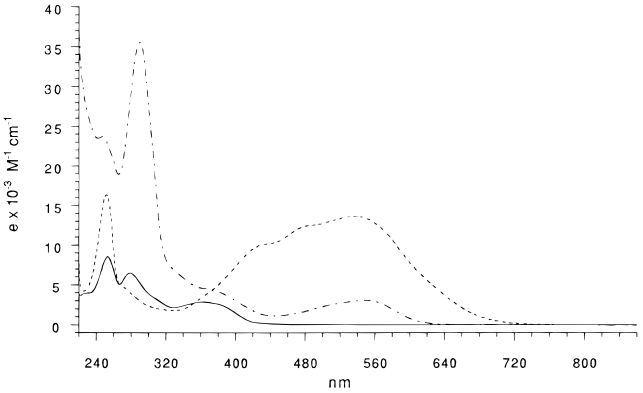

Figure 2. UV−visible spectra of $TcCl_2(Me_2bpy)_2]OTf$ (**3**) (−.−), $TcCl_2(py)_4]OTf$ (**8**) (—), and $TcCl_2(py)_4$ (**9**) (- - -).

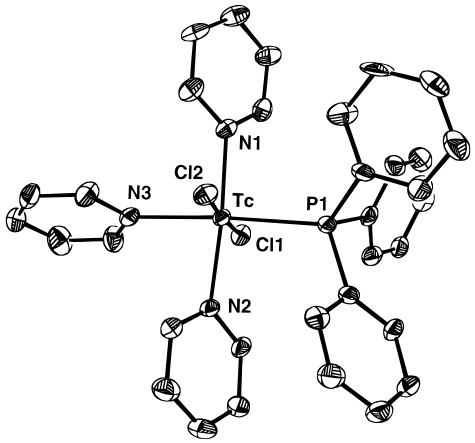

Figure 3. ORTEP representation with 50% probability ellipsoids of $[TcCl_2(py)_3(PPh_3)]PF_6\cdot(CH_2Cl_2)(C_6H_{14})_{1/2}$ (**4**). Hydrogen atoms, solvent molecules, and the PF_6^- ion are omitted for clarity.

290 nm, and the visible portion of the spectrum consists of two broad absorptions at 376 and 549 nm. The most striking observation, however, is the dramatic differences in the UV−visible spectra of $[TcCl_2(py)_4]^+$ and $TcCl_2(py)_4$, Figure 2. The latter exhibits a spectrum similar to that of *cis*-$[Os(NH_3)_4(pz)_2]^{2+}$,[15] with a sharp transition at 252 nm and a highly structured absorption near 540 nm with two strong shoulders to higher energy.

Solid-State Structure. The solid-state structures of $[TcCl_2(py)_3(PPh_3)]PF_6$, $TcCl_2(py)_4$, and $TcCl(tpy)(py)_2$ are shown in Figures 3−5. Selected bond distances and angles for these complexes are listed in Tables 3−5, crystallographic data is shown in Table 6, and selected atomic coordinates are listed in Tables 7−9. The complex *trans*-$[TcCl_2(py)_3(PPh_3)]PF_6$ exhibits an essentially octahedral environment around technetium, with the two *trans*-pyridine ligands bent slightly away from the bulky *cis*-triphenylphosphine ligand (N1−Tc−N2 = 175.6°). The observed Tc−N bond distances of 2.166(5) and 2.165(5) Å, for the pyridine ligands *cis* to triphenylphosphine, are slightly longer (approximately 0.02 Å) than those of the neutral $TcCl_3(pic)_3$ (pic = picoline) and $TcCl_3(pic)(PMe_2Ph)$[5] complexes. The pyridine *trans* to the phosphine exhibits a longer Tc−N bond length of 2.218(5) Å. Typical Tc^{III}−Cl and Tc^{III}−P bond distances of 2.33 average and 2.47 Å, respectively, are observed.[16]

The technetium atom in $TcCl_2(py)_4$ is surrounded by a nearly perfect octahedral arrangement of donor atoms. The Tc−N bond distance of 2.104(2) Å is slightly shorter (0.04 Å) and the

(15) Lay, P. A.; Magnuson, R. H.; Taube, H. *Inorg. Chem.* **1988**, *27*, 2848.
(16) Melník, M.; Van Lier, J. E. *Coord. Chem. Rev.* **1987**, *77*, 275.

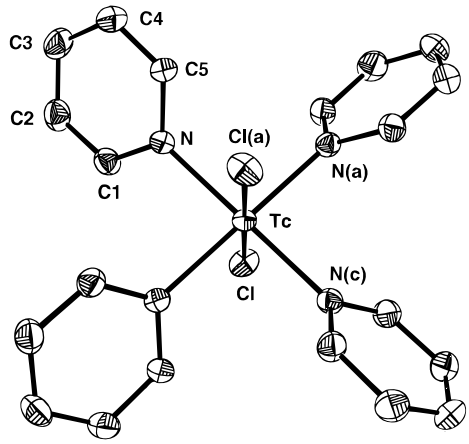

Figure 4. ORTEP representation with 50% probability ellipsoids of $TcCl_2(py)_4$ (**9**). Hydrogen atoms are omitted for clarity.

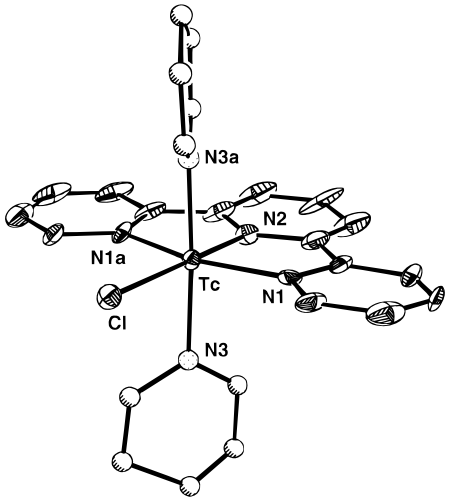

Figure 5. ORTEP representation with 50% probability ellipsoids of $TcCl(tpy)(py)_2\cdot(C_7H_8)$ (**10**). Isotropically refined atoms are represented by shaded (carbon) or dotted (nitrogen) circles; hydrogen and one of each pair of disordered atoms are omitted for clarity.

Table 3. Selected Bond Distances and Angles for $[TcCl_2(PPh_3)(py)_3]PF_6$ (**4**)

Bond Distances (Å)			
Tc−Cl(1)	2.314(1)	Tc−N(1)	2.166(5)
Tc−Cl(2)	2.347(1)	Tc−N(2)	2.165(5)
Tc−P(1)	2.472(2)		
Tc−N(3)	2.218(5)		
Bond Angles (deg)			
Cl(1)−Tc−Cl(2)	176.5(1)	N(1)−Tc−N(3)	90.2(2)
Cl(1)−Tc−P(1)	89.9(1)	N(2)−Tc−N(3)	85.4(2)
Cl(2)−Tc−P(1)	86.8(1)	P(1)−Tc−N(3)	176.6(1)
Cl(1)−Tc−N(2)	90.4(1)	N(1)−Tc−N(2)	175.6(2)
Cl(1)−Tc−N(1)	89.1(1)	P(1)−Tc−N(1)	93.2(1)
Cl(2)−Tc−N(1)	89.7(1)	P(1)−Tc−N(2)	91.1(1)
Cl(2)−Tc−N(2)	91.0(1)		

Table 4. Selected Bond Distances and Angles for $TcCl_2(py)_4$ (**9**)

Bond Distances (Å)			
Tc−Cl	2.407(1)	Tc−N	2.104(2)
Bond Angles (deg)			
Cl−Tc−N	90.5(1)	Cl−Tc−Cl	180.0(1)
Cl−Tc−Na	89.5(1)	N−Tc−Nc	178.9(1)

observed Tc−Cl bond distance of 2.407(1) Å is significantly longer (0.08 Å) in this Tc^{II} complex than are the respective distances in neutral Tc^{III} pyridine complexes.[5]

An octahedral coordination environment also surrounds the technetium atom in $TcCl(tpy)(py)_2$ with the exception of the

Table 5. Selected Bond Distances and Angles for $TcCl(tpy)(py)_2$ (**10**)

	Bond Distances (Å)		
Tc−N1	2.075(6)	Tc−N3	2.136(6)
Tc−N2	1.915(7)	Tc−Cl	2.518(2)
	Bond Angles (deg)		
Cl−Tc−N1	100.9(2)	Cl−Tc−N3	89.3(2)
Cl−Tc−N2	180.0(1)	N1−Tc−N2	79.1(2)

Table 6. Summary of Crystallographic Data[a]

	4	**9**	**10**
chemical formula	$C_{37}H_{39}Cl_4F_6N_3P_2Tc$	$C_{20}H_{20}Cl_2N_4Tc$	$C_{32}H_{33}ClN_5Tc$
a, Å	12.677(4)	15.641(4)	9.359(3)
b, Å	13.064(4)	16.088(6)	
c, Å	13.103(5)	16.845(6)	18.367(4)
α, deg	110.14(3)		
β, deg	101.12(3)		
γ, deg	96.61(2)		
V, Å^3	1959	4121	2765
Z	2	8	4
formula weight	942.4	486.2	622.0
space group	$P\bar{1}$, No. 2	$I4_1/acd$, No. 142	$C222_1$, No. 20
T, °C	−40	−70	−85
λ, Å	0.710 73	0.710 73	0.710 73
ρ_{calcd}, g cm^{-3}	1.595	1.564	1.482
μ, cm^{-1}	7.83	9.70	6.48
R, R_w[b]	0.0615, 0.1148	0.0373, 0.0290	0.0499, 0.0599

[a] **4** = $[TcCl_2(py)_3(PPh_3)]PF_6 \cdot (CH_2Cl_2)(C_6H_{14})_{1/2}$; **9** = $TcCl_2(py)_4$; **10** = $TcCl(tpy)(py)_2 \cdot (C_7H_8)$. [b] $R = \sum||F_o| - |F_c|/\sum|F_o|$; $R_w = [\sum w(|F_o| - |F_c|)^2/\sum w(F_o)^2]^{1/2}$.

Table 7. Selected Fractional Coordinates ($\times 10^4$) and Isotropic Thermal Parameters[a] for $[TcCl_2(py)_3(PPh_3)]PF_6 \cdot (CH_2Cl_2)(C_6H_{14})_{1/2}$ (**4**)

	x	*y*	*z*	U_{eq}
Tc	2415(1)	2566(1)	2417(1)	19(1)
Cl(1)	2005(1)	1130(1)	678(1)	26(1)
Cl(2)	2731(1)	4057(1)	4144(1)	25(1)
P(1)	1238(1)	3618(1)	1606(1)	20(1)
N(1)	1076(4)	1729(3)	2825(4)	22(2)
N(2)	3831(4)	3323(4)	2048(4)	23(2)
N(3)	3558(4)	1676(4)	3125(4)	26(2)

[a] Equivalent isotropic U_{eq} defined as one-third of the trace of the orthogonalized U_{ij} tensor and given in units of Å$^2 \times 10^3$.

Table 8. Fractional Coordinates ($\times 10^4$) and Isotropic Thermal Parameters[a] for $TcCl_2(py)_4$ (**9**)

	x	*y*	*z*	U_{eq}
Tc	0	2500	1250	18(1)
Cl	1088(1)	1412(1)	1250	29(1)
N	−681(2)	1837(2)	367(1)	22(1)
C(1)	−769(2)	969(2)	388(2)	26(1)
C(2)	−1200(2)	516(2)	−176(2)	33(1)
C(3)	−1570(2)	942(2)	−803(2)	37(1)
C(4)	−1495(2)	1823(2)	−837(2)	35(1)
C(5)	−1048(2)	2238(2)	−249(2)	26(1)

[a] Equivalent isotropic U_{eq} defined as one-third of the trace of the orthogonalized U_{ij} tensor and given in units of Å$^2 \times 10^3$.

small bite angle of the terpyridine ligand (N1−Tc−N1a = 158.2(2)°). The Tc−N bond distances of the terpyridine ligand are shorter than those observed in similar technetium terpyridine complexes, $\{[Tc(Me_2bpy)(tpy)]_2(\mu\text{-}O)\}^{4+}$ [17] and $[TcBr(tpy)(PMe_2Ph)_2]^+$.[18] The Tc−N2 (internal nitrogen) bond distance of 1.915(7) Å and the Tc−N1 (external nitrogen) bond distance of 2.075(6) Å are significantly shorter (0.09 and 0.06 Å) than those of the Tc^{III} complex and (0.09 and 0.02 Å) of the Tc^{II} complex. In addition, the observed Tc−Cl bond distance of 2.518(2) Å is 0.06 Å longer than the *trans*-picoline Tc−Cl bond in the neutral $TcCl_3(pic)_3$.[5]

(17) Barrera, J.; Bryan, J. C. Manuscript in preparation.
(18) Wilcox, B. E.; Ho, D. M.; Deutsch, E. *Inorg. Chem.* **1989**, *28*, 3917.

Table 9. Selected Fractional Coordinates ($\times 10^4$) and Isotropic Thermal Parameters[a] for $TcCl(tpy)(py)_2 \cdot (C_7H_8)$ (**10**)

	x	*y*	*z*	U_{eq}
Tc	0	2326(1)	7500	14(1)
Cl	0	760(1)	7500	22(1)
N(1)	−2022(7)	2570(4)	7088(3)	19(2)
N(2)	0	3517(5)	7500	21(3)
N(3)	−890(7)	2266(5)	8570(3)	18(1)

[a] Equivalent isotropic U_{eq} defined as one-third of the trace of the orthogonalized U_{ij} tensor and given in units of Å$^2 \times 10^3$.

Discussion

The synthetic results described above confirm that substitution of both the phosphine and chloride on $TcCl_3(PPh_3)_2(CH_3CN)$ is rather facile relative to $ReCl_3(PPh_3)_2(CH_3CN)$.[19] This is to be expected since metal−ligand bond strengths are in general greater for third-row metals. For example, the reaction of TlOTf and $TcCl_3(PPh_3)(CH_3CN)$ in refluxing pyridine results in the cationic $[TcCl_2(py)_4]OTf$, after 3 h, while this reaction does not occur for rhenium. In addition, $ReCl_3(py)_3$ cannot be prepared directly from $ReCl_3(PPH_3)_2(CH_3CN)$ or $ReCl_3(py)_2(PPh_3)$; rather the $ReCl_3(PPh_3)$(benzil) complex must be utilized to remove the remaining phosphine ligand.[1] In this case the benzil complex may possibly function as a masked Re^V species through the resonance form, $ReCl_3(PPh_3)(PhC(O)=C(O)Ph)$.

The positive shifts in the $Tc^{III/II}$ redox couples upon the substitution of terpyridine or bipyridine for pyridine suggest that the polypyridyl ligand(s) can stabilize Tc^{II}, relative to Tc^{III}, to a greater extent than can a comparable number of pyridine ligands. Thus, an attempt to electrochemically categorize the above technetium complexes according to Lever's ligand electrochemical series was unsuccessful.[13,20] Similar results are observed for the series of complexes $[ReCl(en)_2(L)]^+$, L = substituted pyridine,[2a] as well as for $WCl_2(PMe_3)_2L_2$, $L_2 = (py)_2$ or bipy.[21] These discrepencies apparently arise from the dramatic increase in the π-basicity of Tc^{II} relative to Tc^{III}. This trend is displayed in Figure 6 where the terpyridine complexes exhibit a positive shift of approximately 400−300 mV in the III/II redox couple relative to the analogous pyridine complexes. Interestingly, however, this trend is not observed for the II/I redox couple where the difference in redox potentials of $TcCl(tpy)(py)_2$ and $[TcCl(py)_5]^+$ is only 0.02 mV. In addition, the data in Figure 6 indicates that the slopes of the technetium pyridine complexes generated by the observed III/II and II/I redox potentials (black diamonds) are less, i.e. 0.92 and 0.91, respectively, than the calculated slopes generated by Lever's ligand parameteriztion analysis (open circles).[13,22] The slope values used to generate the calculated data are 1.28 and 1.42, which were derived from Clarke's investigation of various Tc^{III}

(19) Orth. S. D.; Sabat, M.; Harman, W. D. Unpublished results.
(20) Previously Clarke has utilized Lever's analysis to determine the slope and *y*-intercept parameters from a series of known technetium redox values. Assignment of these parameters to $TcCl_3(py)_3$ and $TCl_3(tpy)$ results in ligand parametercs for py and tpy of 0.27 and 0.39, respectively. Lever's analysis indicates no variation in redox potentials for the substitution of polypyridyl ligands for comparable number of pyridine ligands. Py = 0.25; Me_2bpy = 0.23; tpy = 0.25. In addition, Lever warns the reader that his electrochemical parametrization procedure should be used with caution if there are "extraoordinary synergistic interactions between metal and ligand."
(21) Barrera, J.; Sabat, M.; Harman, W. D. *Organometallics* **1993**, *12*, 4381.
(22) Lever, A. B. P. *Inorg. Chem.* **1991**, *30*, 1980.

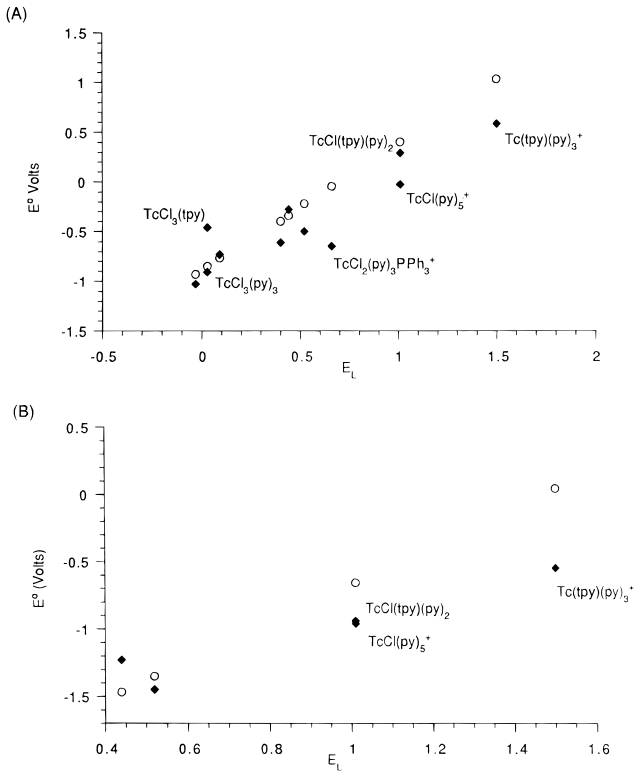

Figure 6. Plots of calculated (open circles) and observed (black diamonds) redox potentials (V vs NHE) vs the sum of ligand parameters E_L: (A) III/II redox couples and (B) II/I redox couples.

pyridine and Tc^{III} phosphine complexes.[5] Thus, it is not surprising to find that the observed data fits the calculated data quite well for several Tc^{III} complexes with pyridine and two to three chloride ligands. However, substitution of the chloride ligands with additional pyridine or polypyridine ligands causes significant differences between the two data sets. First, the smaller value of the observed slope suggests that the substitution of additional pyridine or polypyridine ligands for chloride stabilizes the lower oxidation states to a greater degree than that predicted by Lever's analysis. This is to be expected since the ligand parameter for pyridine or terpyridine was generated from a series of compounds with relatively strong π-acid ligand environments. Second, the nearly identical slope values for both the $Tc^{III/II}$ and $Tc^{II/I}$ couples suggests that the electronic characters of Tc^{II} (d^5) and Tc^{I} (d^6) metal centers with a predominantly pyridine ligand environment are surprisingly quite similar. This observation is supported by the nearly identical $Tc^{II/I}$ redox couples for $[TcCl(py)_5]^+$ and $TcCl(tpy)(py)_2$. However, this does not suggest that the total extents of Tc−pyridine π-back-bonding for both complexes are similar. A greater π-interaction is expected in the case of $TcCl(tpy)(py)_2$; however, in this compound the π-back-bonding is dominated by the terpyridine ligand rather than by the two pyridine ligands. This electrochemical evidence is supported by the structural data of $TcCl(tpy)(py)_2$ and $TcCl_2(py)_4$ (*vide infra*).

The UV−visible spectra of the Tc^{III} pyridine complexes are similar to those of the corresponding Tc^{III} and Tc^{II} phosphine complexes reported by Deutsch.[4] The latter exhibit transitions between 400 and 500 nm that were assigned as halide-to-metal charge transfer due to their respective blue shift upon reduction and substitution of bromide by the weaker reductant chloride. The low-energy transitions in the Tc^{III} pyridine complexes are also assigned as halide to metal; however, they are significantly higher in energy than those of the corresponding phosphine complexes. The transitions at 253 nm in **7**−**9** are assigned as a pyridine-localized $\pi-\pi^*$ transition on the basis of the energy and intensity of such transitions in free pyridine and $[(NH_3)_5Ru(py)]^{n+}$.[23] Finally, the dramatic spectral differences that exist between $[TcCl_2(py)_4]^+$ and $TcCl_2(py)_4$ deserve comment. In the case of the latter, the reduced metal center results in a series of three intense transitions between 435 and 540 nm (10100−13600 M^{-1} cm^{-1}). These charge transfer transitions are assigned as metal to pyridine on the basis of similar assignments in $[Ru(py)_6]^{2+}$ [24] and *trans*-$[(NH_3)_4Ru(py)_2]^{2+}$.[25]

The most striking evidence for the electron-rich character of low-valent Tc−amine complexes is the observed structural data. A decrease of 0.04 Å and an increase of 0.07 Å are observed in the *trans*-Tc−N and *trans*-Tc−Cl bond distances, respectively, between the similar technetium complexes *trans*-$TcCl_2(py)_4$ and *mer*-$TcCl_3(pic)_3$. Such structural differences are best explained by the dramatic increase in π-basicity of Tc^{II} relative to Tc^{III}. On the other hand, the observed increase of 0.03 Å in the Tc−N(py) bond distance in $TcCl(tpy)(py)_2$ relative to $TcCl_2(py)_4$ is best explained by the presence of the terpyridyl ligand in the former. In this case the metal should possess greater π-overlap with the flat polypyridyl ligand; hence the need to back-donate into the available pyridine ligands is reduced. This is strongly demonstrated by the 0.09 Å decrease in the Tc−N(internal) bond of the terpyridyl ligand in $TcCl(tpy)(py)_2$ relative to other known Tc^{II} and Tc^{III} terpyridyl complexes.[15,16]

Summary

Substitution of pyridine(s) for either the triphenylphosphine or chloride ligands on $TcCl_3(PPh_3)_2(CH_3CN)$ is quite facile relative to the analogous rhenium compound. As a result, a series of Tc^{III} complexes with pyridine and polypyridine ligands were prepared and characterized by ^1H NMR, UV−visible, and cyclic voltammetry. The Tc^{III} pyridine complexes exhibit Knight-shifted ^1H NMR spectra, transitions in the visible spectra that are tentatively assigned as halide to metal, and multiple reversible electrochemical redox couples.

The electronic spectra, the substitution chemistry, and the X-ray data indicate that significant π-back-bonding interactions exist in the cases of Tc^{II} and Tc^{I} complexes relative to Tc^{III}. Thus, stabilization of the low oxidation states of technetium through pyridine ligation is supported by intense MLCT transitions observed in $TcCl_2(py)_4$ relative to $[TcCl_2(py)_4]^+$, the relative difficulty to substitute the chloride or pyridine in $TcCl_2(py)_4$, the decrease of 0.04−0.06 Å in Tc−N bond lengths between Tc^{III} and Tc^{II} pyridine complexes, and the decrease of 0.09 Å in Tc−N(internal) bond lengths between Tc^{III} and Tc^{I} terpyridine complexes. Finally, the unique electronic flexibility of a coordinated pyridine(s) is demonstrated by the variations in the Tc−N(py) bond lengths for the three different oxidation states of technetium.

Acknowledgment. This work was supported by Laboratory Directed Research and Development and performed under the auspices of the U.S. Department of Energy at Los Alamos National Laboratory.

Supporting Information Available: Listings of bond lengths and angles, atomic coordinates, and thermal parameters and completely labeled diagrams for $[TcCl_2(PPh_3)(py)_3]^+$, $TcCl_2(py)_4$, and $TcCl(tpy)(py)_2$ (26 pages). Ordering information is given on any current masthead page.

IC950291Q

(23) Ford, P.; Rudd, De F. P.; Gaunder, R.; Taube, H. *J. Am. Chem. Soc.* **1968**, *90*, 1187.
(24) Templeton, J. L. *J. Am. Chem. Soc.* **1979**, *101*, 4906.
(25) Ford, P. C.; Sutton, C. *Inorg. Chem.* **1969**, *8*, 1544.